RSC Advances

PAPER

View Article Online
View Journal | View Issue

Cite this: *RSC Adv.*, 2017, **7**, 3727

Surfactant-assisted preparation of Y_2O_3-stabilized ZrO_2 nanoparticles and their tribological performance in mineral and commercial lubricating oils†

Dandan Li, Yuchen Xie, Huaisong Yong and Dazhi Sun*

Received 5th November 2016
Accepted 20th December 2016

DOI: 10.1039/c6ra26346a

www.rsc.org/advances

We report the synthesis and tribological characterization of zirconia (ZrO_2) nanoparticles in base mineral oil and commercial formulated lubricating oils. A modified chemical method was applied to prepare nano-sized ZrO_2 structurally stabilized with yttria (Y_2O_3) in a precipitation process with the addition of various surfactants (polyethylene glycol, polyvinyl pyrrolidone, and polyether amine). Characterizations by X-ray diffraction and transmission electron microscopy show that polyether amine facilities the formation of stable ZrO_2 with coexisting tetragonal and monoclinic phases and is better in preparing Y_2O_3-stabilized ZrO_2 nanoparticles with a smaller particle size and narrower size distribution compared to the other surfactants used. The friction and anti-wear characteristics, which were tested with a four-ball module, indicate that the as-prepared Y_2O_3-stabilized ZrO_2 nanoparticles perform better in commercial formulated lubricating oils than in the base mineral oil medium, and 0.1–0.5 wt% nanoparticles should be sufficient to achieve good tribological performance in lubricating oils.

1. Introduction

The addition of inorganic nanoparticles into lubricating oils has attracted extensive attention both in the scientific community and in the lubrication industry because of its effectiveness in reducing wear and friction. Varieties of inorganic nanomaterials including metal nanoparticles, metal oxide nanoparticles, carbon nanomaterials, and metal dichalcogenide nanostructures have been utilized in oil media to improve the anti-wear and friction-reduction properties.[1–10] Among the inorganic nanoparticles utilized in lubricating oils, metal oxide nanoparticles possess advantages such as low cost, relatively high stability, and ease of controlling the particle size and morphology, making them good candidates for commercial applications in lubricating oils.

The use of common metal oxide nanoparticles such as Al_2O_3, MgO, ZnO, CuO, and TiO_2 in lubricating oils has been frequently studied in the literature. Wu and co-workers[11] examined the tribological properties of lubricating oils with various nanoparticles, including CuO, TiO_2, and nano-diamond, all of which exhibit good friction-reduction and anti-wear behaviors, particularly CuO. In the study of Ingole and co-workers,[12] nano-sized TiO_2 particles prepared by co-precipitation had a minor reduction effect on the coefficient of friction of the base oil. Luo and co-workers[13] prepared homogeneously dispersed Al_2O_3 nanoparticles using silane coupling agents. When 0.1 wt% of Al_2O_3 nanoparticles were added into the base oil, the friction and anti-wear properties were markedly improved. Later, the same team[14] found that Al_2O_3/TiO_2 nanocomposites provided a much better tribological performance than pure Al_2O_3 or TiO_2.

Compared with other metal oxides, ZrO_2 is highly crystalline, chemically resistant, and extra-hard. However, the utilization of ZrO_2 nanoparticles in lubricating oils is not yet well-understood. Only a few studies on the applications of ZrO_2 in lubricating oils have been reported. Battez and co-workers[15] discussed the wear-prevention behavior of metal oxide nanoparticles, including CuO, ZrO_2 and ZnO nanoparticles, in oil under extreme pressure, and all the nanoparticles resulted in improved properties. In their work, monoclinic ZrO_2 was spherical, with a diameter of 20–30 nm, and the wear scar diameter was the lowest when the ZrO_2 nanoparticle concentration reached about 2 wt%. They also proposed that the good results under extreme pressure were related to the size and hardness of the nanoparticles. Later on, the same group reported the anti-wear behaviors of these three nanoparticles.[16] In their study, base oil containing 0.5 wt% ZrO_2 nanoparticles exhibited the best tribological behavior. They suggested that both the friction and anti-wear behaviors are important in the design of lubricating oil formulations because both parameters may show different tendencies depending on the nanoparticle

Department of Materials Science and Engineering, Shenzhen Key Laboratory of Nanoimprint Technology, Southern University of Science and Technology, Shenzhen 518055, China. E-mail: sundz@sustc.edu.cn

† Electronic supplementary information (ESI) available. See DOI: 10.1039/c6ra26346a

concentration. Moreover, Zr-based bulk metallic glasses used for hard-tissue replacements have tremendous potential because of their low friction coefficients and wear resistances compared to conventional CoCrMo alloy.[17] ZrO_2-toughened alumina ceramic composites show better wear resistance than Al_2O_3.[18] Alumina ceramics containing Zr additives exhibited higher wear resistances and lower friction coefficients.[19] These studies suggest that zirconium compounds may be excellent candidates as anti-wear and friction-reduction additives.

Pure zirconia typically exhibits three types of crystal structures, monoclinic, tetragonal and cubic, the last of which is less common. The use of pure ZrO_2 is limited by its spontaneous stress-induced martensitic transformation from tetragonal to monoclinic during the cooling process. While monoclinic zirconia is less desirable because of its phase instability, the retention of the tetragonal phase at room temperature is essential to increase the mechanical integrity of ZrO_2 (ref. 20), and stabilized and toughened zirconia ceramics thus show great potential for various anti-wear applications.[21] ZrO_2 can be stabilized by doping with MgO, CaO, Al_2O_3, Y_2O_3, and others; among these, yttria-stabilized zirconia (YSZ) is frequently used.[22] It has been suggested that upon the addition of a few percent of Y_2O_3 (3–5 mol%), most of the ZrO_2 crystals can be stabilized in the tetragonal phase during the cooling process after calcination. Such stabilized zirconia with coexisting tetragonal and monoclinic phases would exhibit balanced hardness and toughness.[23]

Various methods have been reported to prepare YSZ microparticles and nanoparticles, such as co-precipitation,[23] hydrothermal synthesis,[24,25] and sol–gel processes.[26] Because of the ease of operation and low cost, the co-precipitation process has been widely used in both research labs and industries. However, the use of surfactants to control the quality of YSZ particles, particularly nanoparticles, has not yet been widely adopted. In this paper, we report the controlled synthesis of 3 mol% yttria-stabilized zirconia (3YSZ) nanoparticles with coexisting tetragonal and monoclinic phases through a precipitation method with various surfactants. We then report the tribological properties of the as-prepared 3YSZ nanoparticles in oils. Previous research on nanoparticle-bearing lubricating oils has focused on the friction and anti-wear properties in base oil media, such as mineral oils and synthetic oils. The lubricating behaviors of nanoparticles, particularly 3YSZ nanoparticles, in commercial formulated oils have not yet been studied in detail; therefore, our current work initiates the discussion on the potential utilization of synthetic metal oxide nanoparticles in commercial formulated lubricating oils.

2. Experimental

2.1 Synthesis and characterization of 3YSZ nanoparticles

Zirconyl chloride octahydrate ($ZrOCl_2 \cdot 8H_2O$ purity ~ 98%, supplied by Aladdin, China) and yttrium nitrate hexahydrate ($Y(NO_3)_3 \cdot 6H_2O$, purity ~ 99.5%, supplied by Aladdin, China) were used in this study. $ZrOCl_2 \cdot 8H_2O$ and $Y(NO_3)_3 \cdot 6H_2O$ were first dissolved in deionized water. The molar ratio of Y_2O_3 to (Y_2O_3 + ZrO_2) was fixed at 3 mol%. Next, 1 wt% polyethylene glycol (PEG-4000), polyvinyl pyrrolidone (PVP-10 000), or polyether amine D2000 (industrial grade) was added into the mixture as a surfactant to reduce agglomeration. Each solution was mixed using a magnetic stirrer and heated to 75 °C in a thermostatic bath. Subsequently, ammonia aqueous solution (25%, Guangzhou chemical regent factory, China) was slowly added into the above mixture until the pH reached ~9. After two hours of reaction, the precipitates were collected and rinsed repeatedly with deionized water to remove the unwanted ions. The washing was monitored with $AgNO_3$ solution and carried out until no AgCl precipitation occurred. The purified precipitates were dried overnight at 110 °C in an oven and finally calcined in a furnace at various temperatures for different durations to obtain 3YSZ nanoparticle powders. A sample without any surfactant was also prepared for comparison and designated as sample I. The samples with PEG-4000, polyether amine D2000, and PVP-10 000 were designated as sample II, sample III, and sample IV, respectively. Elemental analyses of samples I–IV showed that the surfactants and absorbing molecules were completely removed after calcination (Fig. S1 in ESI†).

The crystalline phases of the calcined 3YSZ nanoparticles were identified by X-ray diffraction (XRD; D8 Advance, Bruker, Germany) with Cu Kα radiation and a Ni filter operating at 40 kV and 40 mA. The grain sizes of the nanoparticles were determined using the Scherrer equation through the line-broadening method:

$$d_{XRD} = \frac{0.89\lambda}{B\cos\theta}, \quad (1)$$

where d_{XRD} is the crystallite size of the tetragonal ZrO_2 phase, B represents the diffraction peak width measured at half the maximum intensity, $\lambda = 1.5405$ Å is the wavelength of the X-ray radiation, and θ is the Bragg angle. The tetragonal reflection at $2\theta = 30.1^\circ$ was used to roughly estimate the crystallite sizes of the YSZ nanoparticles.

Micrographic images of the calcined 3YSZ nanoparticles were obtained by transmission electron microscopy (TEM; Tecnai F30, Philips-FEI, Holland) operating at 300 kV.

2.2 Preparation of lubricating oils with 3YSZ nanoparticles

In this work, mineral oil and commercial lubricating oils for car engines, including KR7 (supplied by China Petroleum) and Mobil 1 (supplied by ExxonMobil), were purchased directly from the market. 3YSZ nanoparticles at different concentrations were dispersed in each lubricating oil with 1.0 wt% of poly(isobutene-*b*-propylene oxide-*b*-isobutene) block copolymer prepared in our lab by mechanical agitation and ultra-sonication for about 10 min before tribological testing.

2.3 Friction and anti-wear testing method

The friction and anti-wear properties of the prepared lubricating oils were estimated using a Bruker UMT-2 equipped with a four-ball test setup. Before each test, the ball holder was washed with petroleum ether, and the balls were cleaned ultrasonically in ethyl alcohol and thoroughly air-dried. Three

Table 1 Testing conditions

Type of oil	Mass ratio of 3YSZ nanoparticles in oil			Load carrying capacity (N)	Revolution per minutes (rpm)
Base oil	0.1%	0.5%	1.0%	14.7; 40; 80	200; 400
KR7	0.1%	0.5%	1.0%	80	400
Mobil 1	0.1%	0.5%	1.0%	80	400

stainless-steel balls with diameters of 12.7 mm were clamped together in the groove and covered with about 10 mL of lubricating oil. A fourth ball (diameter = 12.7 mm), referred to as the top ball, was pressed into a holder. The tester was operated with one steel ball held stationary against three steel balls under load and rotating in the form of a cradle at room temperature. The testing conditions are listed in Table 1. The friction coefficient was recorded by means of a load transducer positioned to measure the lateral force. Wear surfaces were characterized using a Leica DM2700M microscope.

3. Results and discussion

3.1 Synthesis and characterization of 3YSZ nanoparticles

Fig. 1 illustrates the XRD patterns of the 3YSZ nanoparticles synthesized by calcining the dried precursor powders at different temperatures within the range of 500–900 °C for 2 h. The dried precursor powders were prepared by drying the precipitates after reaction with and without surfactants at 110 °C. For all the samples prepared with and without surfactants, the dried precursors after heating at 110 °C were amorphous, as indicated by the absence of any XRD peaks in the spectra shown in Fig. 1(a)–(d). After calcination at 500 °C, the tetragonal phase was observed in all four samples, and monoclinic crystals appeared only in sample IV. The weak and broad monoclinic diffractions in Fig. 1(d) indicate poor crystallinity and very small crystallite size.[27] After calcination at 600 °C, the monoclinic phase began to appear in sample III [Fig. 1(c)], whereas only the tetragonal phase was observed in samples I and II [Fig. 1(a) and (b), respectively]. When the calcination temperature was increased to 700 °C, the monoclinic phase appeared in sample I [Fig. 1(a)], whereas sample II still only contained the tetragonal phase [Fig. 1(b)]. The monoclinic and tetragonal phases coexisted when the samples were calcined at temperatures higher than 700 °C (Fig. 1). The above results demonstrate that the addition of surfactants during the precipitation process affects the monoclinic crystal formation temperature during the calcination of YSZ. In sample II, the added PEG-4000 retarded the growth of the monoclinic phase in the 3YSZ nanoparticles, while the polyether amine D2000 and PVP-10 000 facilitated the formation of monoclinic crystals, thus allowing tetragonal and monoclinic nanocrystals to coexist at a lower calcination temperature. Moreover, the intensities of the XRD peaks increased as the calcination temperature increased from 500 °C to 900 °C, indicating that highly crystalline 3YSZ nanoparticles can be obtained by increasing the calcination temperature, which agrees with the literature.[28] Fig. 1 also shows that the crystallites exist as either tetragonal ZrO_2 or coexisting tetragonal and monoclinic ZrO_2 rather than solely monoclinic ZrO_2.[29] The monoclinic portions in sample III and sample IV are greater than those in sample I and sample II at the same temperature, suggesting that structurally stable 3YSZ nanoparticles can be prepared using polyether amine D2000 and PVP-10 000 as surfactants. Such high-quality 3YSZ nanoparticles are suitable for investigating lubricating performance in oil media.

The average crystallite sizes of all samples were determined by XRD from the Scherrer equation, as shown in eqn (1), and are plotted in Fig. 2. The average nanoparticle size increased with increasing calcination temperature. The average nanoparticle sizes for sample II with PEG-4000 as the surfactant were larger than those for sample I without any surfactant at every temperature studied from 500–900 °C. Sample III with polyether amine D2000 as surfactant and sample IV with PVP-10 000 as surfactant had smaller nanoparticles sizes than sample I without any surfactant. Comparing the average nanoparticle sizes in Fig. 2 and the temperature-dependent crystalline phase formation results shown in Fig. 1 suggests that the formation of the monoclinic phase, which is induced by the addition of surfactants such as polyether amine and PVP, helps reduce the 3YSZ nanoparticle size during the calcination process.

The average nanoparticle size and size distribution were also analyzed directly by electron microscopy. Fig. 3 shows typical TEM images of 3YSZ nanoparticles in samples I–IV calcined at 900 °C. The average nanoparticle size for all the prepared samples was about 30 nm, but only sample III exhibited a relatively narrow size distribution. The statistical analysis based on about 200 nanoparticles from the TEM images for each sample is shown in Fig. 4. Sample I without any surfactant showed an average particle size of 31.8 nm, with a standard deviation of ±10.4 nm, while sample II with PEG-4000 showed a larger particle size of 36.9 nm and a slightly narrower size distribution of ±9.1 nm. The comparison of the TEM images and statistical analysis between sample I and sample II suggests that PEG is inefficient at reducing the average size and size distribution of 3YSZ nanoparticles in the precipitation method, which agrees with the XRD results shown in Fig. 2. Sample III with polyether amine D2000 and sample IV with PVP-10 000 showed average particle sizes of 26.8 ± 8.0 nm and 30.0 ± 11.2 nm, respectively, indicating that both polyether amine and PVP can help reduce the 3YSZ nanoparticle size, and that among the surfactants studied in this work, polyether amine is the most efficient at preparing small 3YSZ nanoparticles. Polyether amine was also the best surfactant for synthesizing uniform 3YSZ nanoparticles in the current study. Therefore, sample III (3YSZ nanoparticles prepared with polyether amine D2000) was utilized as model 3YSZ nanoparticles to study the friction and anti-wear behaviors in various lubricating oils.

3.2 Lubricating behaviors of 3YSZ nanoparticles in base oil and commercial formulated lubricating oils

Fig. 5 shows the friction coefficients as a function of time up to 1 h for base mineral oils containing various concentrations of

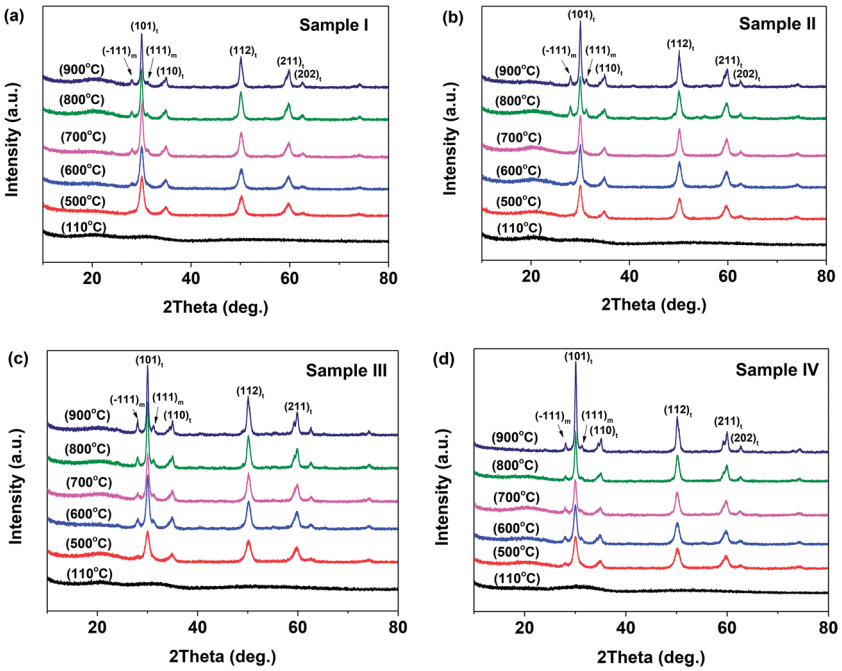

Fig. 1 XRD patterns of 3YSZ before and after calcining at various temperatures: (a) sample I, (b) sample II, (c) sample III, and (d) sample IV. "t" and "m" represent the tetragonal and monoclinic zirconia, respectively. Sample I represents the sample without any surfactant, and the samples with PEG-4000, polyether amine D2000, and PVP-10 000 are assigned as sample II, sample III, and sample IV, respectively.

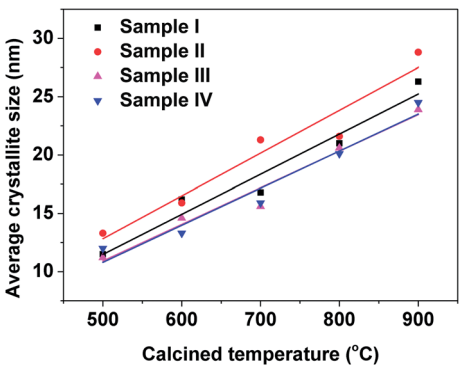

Fig. 2 Average crystallite sizes (determined by XRD) of the 3YSZ nanoparticles prepared by calcining the dried precursor powders at various temperatures for 2 h.

3YSZ nanoparticles from sample III with increased load and rotational speed under our four-ball testing experiments. The testing conditions are summarized in Table 1. Under the mild testing condition with a load of 14.7 N and a rotational speed of 200 rpm, the base oils containing 0.1, 0.5, and 1.0 wt% 3YSZ nanoparticles all showed higher friction coefficients than the base mineral oil, as shown in Fig. 5(a). This indicates that the 3YSZ nanoparticles are unable to reduce the friction coefficient of the base mineral oil under light-load and slow-rotation conditions. When the load and rotational speed were increased to 40 N and 400 rpm, respectively, the base oil with 0.1 wt% of 3YSZ nanoparticles still showed a higher friction coefficient than the base oil alone, as illustrated in Fig. 5(b). However, Fig. 5(b) also shows that the friction coefficient of the base oil containing 0.5 wt% 3YSZ nanoparticles was about 10% lower than that of the control oil, and the friction coefficient of the base oil with 1.0 wt% 3YSZ nanoparticles was similar to that of the base oil alone. Fig. 5(c) shows the results for a load of 80 N and a rotational speed of 400 rpm. Under these testing conditions, all the oil samples containing 3YSZ nanoparticles showed lower friction coefficients than the control base oil, and the friction coefficient decreased with increasing nanoparticle

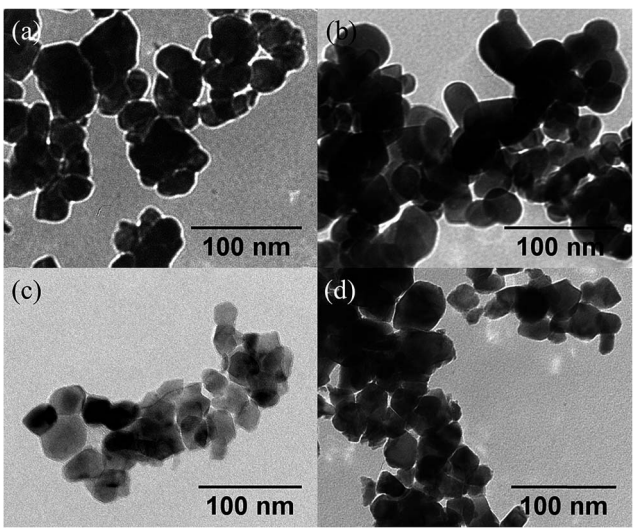

Fig. 3 TEM images of 3YSZ nanoparticles prepared (a) without any surfactant (sample I) and with (b) PEG-4000 (sample II), (c) polyether amine D2000 (sample III), and (d) PVP-10 000 (sample IV) as surfactants.

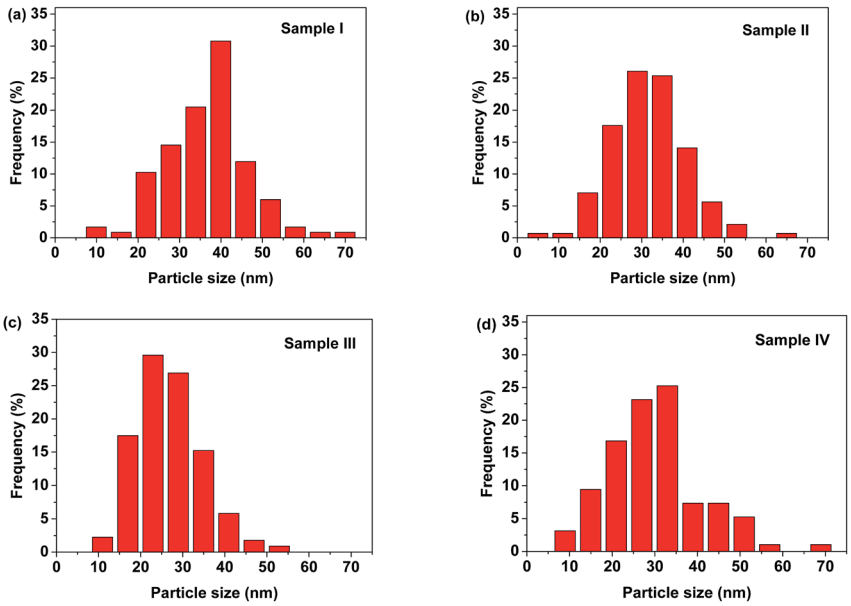

(e)

	Sample I	Sample II	Sample III	Sample IV
Average d (nm)	31.8±10.35	36.88±9.12	26.82±7.97	30.04±11.17

Fig. 4 Size distributions of 3YSZ nanoparticles prepared with and without surfactants after calcination at 900 °C for 2 h: (a) sample I, (b) sample II, (c) sample III, and (d) sample IV. Sample I represents the sample without any surfactant, and the samples with PEG-4000, polyether amine D2000, and PVP-10 000 as surfactants are designated as sample II, sample III, and sample IV, respectively. (e) Table showing the results of statistical analysis.

concentration. Fig. 5(c) shows that all the lubricating oils containing 3YSZ nanoparticles showed unusually high friction coefficients at the early stage of the four-ball testing, which is probably attributable to the existence of nanoparticle clusters. Under a relatively heavy load, these clusters began to disaggregate rapidly between the rotating metal balls, after which the

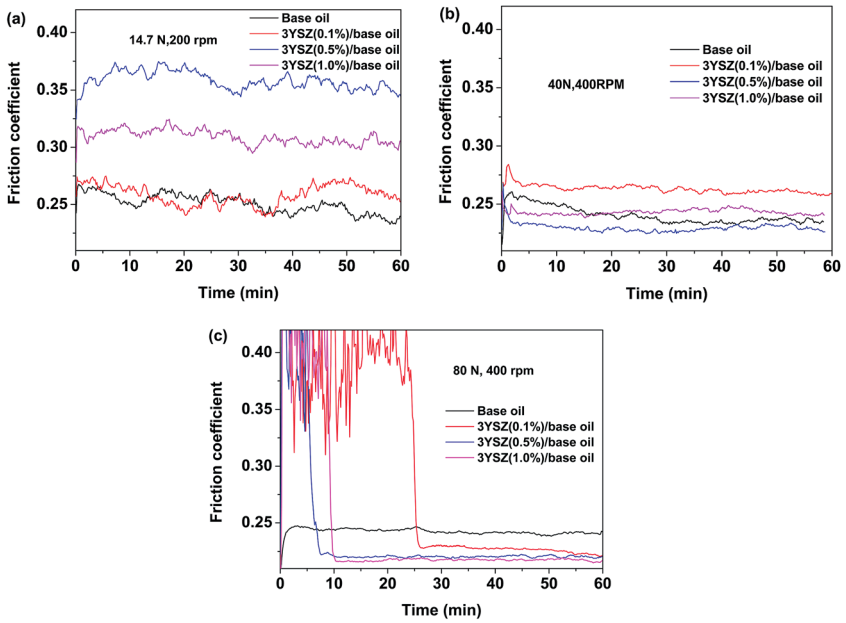

Fig. 5 Friction coefficients as functions of time for the base oils with various concentrations of 3YSZ nanoparticles under different testing conditions: (a) 14.7 N and 200 rpm, (b) 40 N and 400 rpm, and (c) 80 N and 400 rpm.

friction coefficients returned to normal and remained stable. Moreover, as shown by comparing Fig. 5(a)–(c), the friction coefficient of the control base oil remained nearly the same at ~0.250 under different testing conditions, while the mineral oils with added 3YSZ nanoparticles showed reduced friction coefficients as the testing load and rotational speed increased. The lowest friction coefficient for a mineral oil sample containing 3YSZ nanoparticles tested in our experiments was ~0.210 under 80 N and 400 rpm, which represents an approximately 16% reduction compared to the base mineral oil. The above phenomenon also illustrates that 3YSZ nanoparticles in the base oil are efficient at lubricating the interface between metals under heavy-load and high-frictional-speed conditions. This may be attributed to the high hardness and high stability of 3YSZ nanoparticles with a majority of tetragonal phase compared to other types of zirconia.[30]

To test the tribological performances of our 3YSZ nanoparticles in formulated oils, two commercial lubricating oils, one Chinese brand from PetroChina (KR7) and one US brand from ExxonMobil (Mobil 1) were purchased directly from the market and utilized in the current study. Fig. 6(a) and (b) show the friction coefficients of KR7 and Mobil 1 with and without the addition of 3YSZ nanoparticles under a load of 80 N and a rotational speed of 400 rpm, respectively. In Fig. 6(a), KR7 and KR7 containing 0.1 and 0.5 wt% 3YSZ nanoparticles show similar friction coefficients of ~0.165, and KR7 with 1.0 wt% 3YSZ nanoparticles possesses a higher friction coefficient of ~0.185, indicating that 3YSZ nanoparticles are incapable of enhancing the lubricating behaviors of KR7, and a higher concentration of 3YSZ nanoparticles may cause a significant increase in the friction coefficient of KR7. In contrast, as shown in Fig. 6(b), the Mobil 1 oils containing 0.1 and 0.5 wt% 3YSZ nanoparticles had friction coefficients of ~0.180 and ~0.175, respectively, lower than that of Mobil 1 without 3YSZ nanoparticles (about 0.210). However, when the concentration of 3YSZ nanoparticles was increased to 1.0 wt% in Mobil 1, the friction coefficient increased to ~0.200, which is slightly lower than that of the control Mobil 1 oil.

The average friction coefficients as functions of the 3YSZ nanoparticle concentration in the base mineral oils KR7 and Mobil 1 measured at 80 N and 400 rpm and derived from Fig. 5(c) and 6 are plotted in Fig. 7. First, the friction coefficients of the base oil, KR7, and Mobil 1 were lower than that of the base oil, mainly because the two commercial oils already contain formulated lubricating agents. Second, the addition of 3YSZ nanoparticles synthesized in the current work reduced the friction coefficients of the base oil, KR7, and Mobil 1 to different extends. For the base mineral oil, the friction coefficient decreased gradually as the concentration of 3YSZ nanoparticles increased, as discussed previously for Fig. 5(c). As for the commercial formulated lubricating oils, our 3YSZ nanoparticles were more efficient in reducing the friction coefficient of KR7 than that of Mobil 1. The KR7 oil did not show a considerable reduction in friction coefficient when 0.1 wt% 3YSZ nanoparticles were added, and the friction coefficient was even slightly increased compared to that of pure KR7 when the concentration of 3YSZ nanoparticles was increased to 0.5 wt%. On the other hand, the Mobil 1 oil experienced significant reductions of about 15% and 17% in friction coefficient when 0.1 wt% and 0.5 wt% 3YSZ nanoparticles were added, respectively. The difference in the reductions in friction coefficient between KR7 and Mobil 1 when less than 0.5 wt% 3YSZ nanoparticles were added can probably be attributed to the two following reasons. (i) Our 3YSZ nanoparticles are more compatible with the Mobil 1 formulation than KR7. The good dispersion of nanoparticles with a relatively low concentration in the oil medium leads to an efficient reduction in the friction coefficient, similar to many observations in the literature.[3–8] (ii) The KR7 formulation may already contain a relatively large amount of lubricating agents; thus the effect of adding 3YSZ

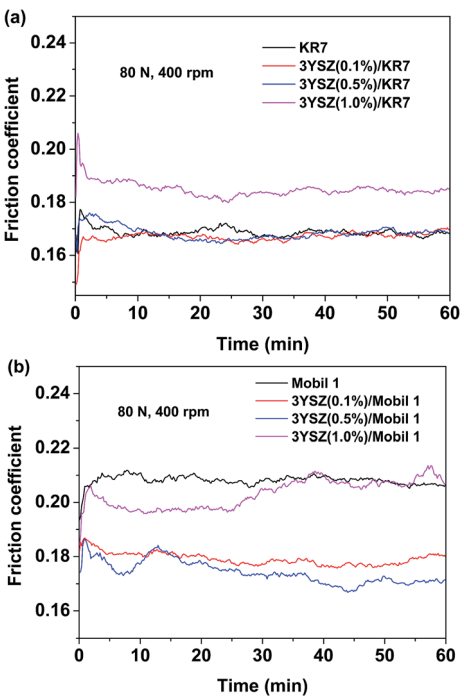

Fig. 6 Friction coefficients of (a) KR7 and (b) Mobil 1 with and without added 3YSZ nanoparticles under a load of 80 N and a rotational speed of 400 rpm.

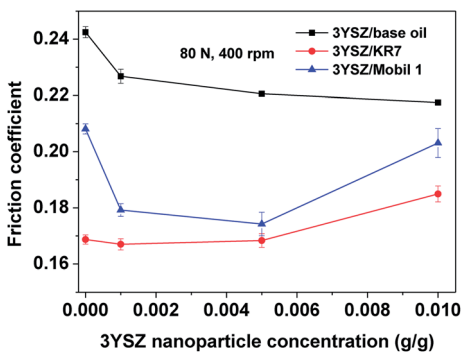

Fig. 7 Comparison of the friction coefficients for different 3YSZ nanoparticle concentrations in the base mineral oil, KR7, and Mobil 1. The tests were performed under a load of 80 N and a rotational speed of 400 rpm for 1 h.

nanoparticles on the friction coefficient is not obvious. Lastly, when the concentration of 3YSZ nanoparticles was increased to 1.0 wt%, both KR7 and Mobil 1 showed higher friction coefficients than the corresponding low-nanoparticle-concentration samples. The friction coefficient of the KR7 oil with 1.0 wt% 3YSZ nanoparticles was 20% higher than that of the pure KR7. This phenomenon may be explained by the fact that a relatively high concentration of nanoparticles results in severe nanoparticle aggregation, resulting in a significant increase in friction coefficient.[8] The above discussion suggests that 0.1–0.5 wt% of our 3YSZ nanoparticles is sufficient to reduce the friction coefficients of lubricating oils.

The wear scar images of the worn metal balls after four-ball testing for 1 h under a load of 80 N and a rotational speed of 400 rpm are shown in Fig. 8. The images for the samples made using the three control oils (the base mineral oil, KR7, and Mobil 1) with and without the addition of 0.5 wt% 3YSZ nanoparticles are shown to demonstrate the anti-wear properties of our 3YSZ nanoparticles in lubricating oils. The average wear scar diameters (WSDs) as functions of 3YSZ nanoparticle concentration in the base mineral oil, KR7, and Mobil 1 are plotted in Fig. 9. The WSD for the base mineral oil was similar to those for KR7 and Mobil 1, but the wear scars for KR7 and Mobil 1 appeared much smoother than those for the base mineral oil, indicating that KR7 and Mobil 1 have good lubricating formulations. For the addition of 3YSZ nanoparticles, the WSD for the base mineral oil containing 0.1 wt% nanoparticles was about five-fold larger than that for the base mineral oil alone, and the WSDs for the base mineral oil containing 0.5 and 1.0 wt% nanoparticles were about three-fold larger. Most previously reported data regarding the addition of ZrO_2 nanoparticles[15,16] and other oxide nanoparticles[3–8] to base oil media indicate different degrees of anti-wear enhancement or sometimes a decrease in wear protection, and such large WSDs for the base oils with 3YSZ nanoparticles have not been seen before. This observation agrees with the corresponding friction coefficient results shown in Fig. 5(c). The unusually large friction coefficients at the early stage of four-ball testing are likely the reason for the formation of such large wear scars. The mechanisms responsible for this phenomenon may be the poor dispersion of 3YSZ nanoparticles in the base oil, as discussed previously for Fig. 5(c), and the fact that the 3YSZ nanoparticles containing

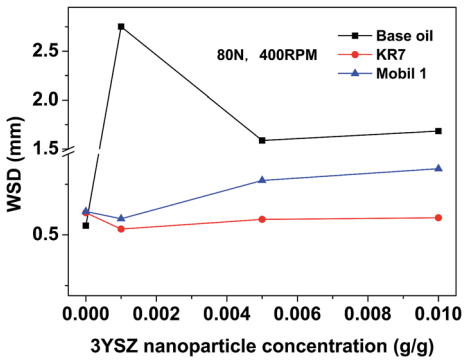

Fig. 9 Average WSD as a function of 3YSZ nanoparticle concentration in the base mineral oil, KR7, and Mobil 1. The tests were performed under a load of 80 N and a rotational speed of 400 rpm for 1 h.

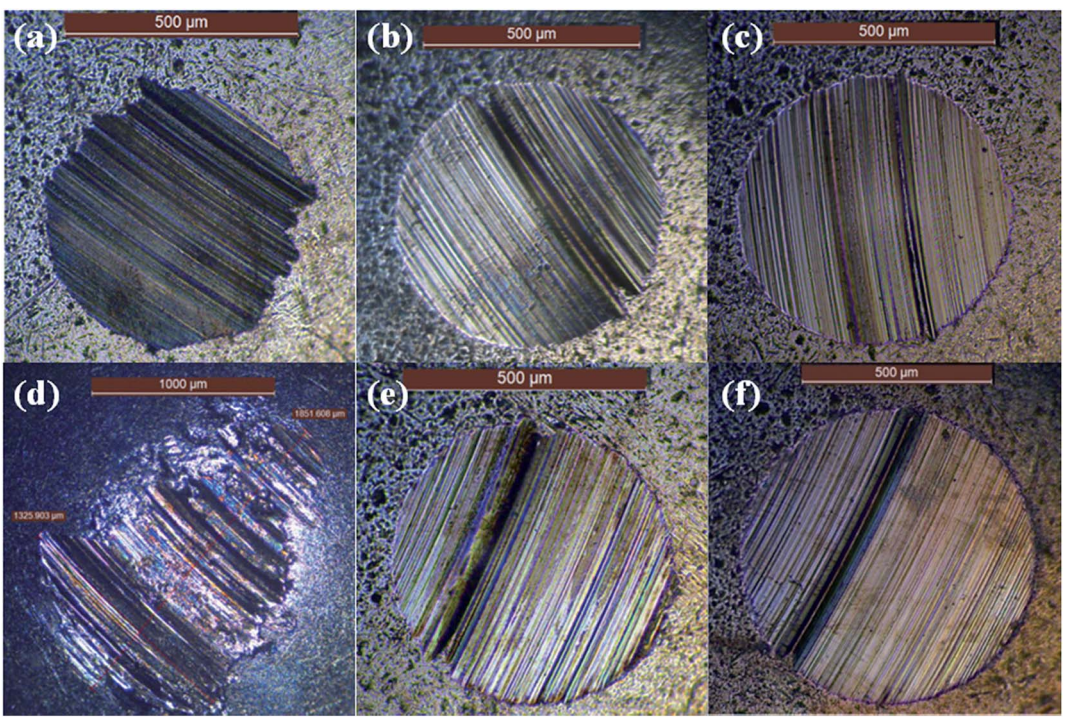

Fig. 8 Wear scar images of the worn metal surfaces after four-ball testing for 1 h under a load of 80 N and a rotational speed of 400 rpm: (a) base oil, (b) KR7, (c) Mobil 1, (d) base mineral oil with 0.5 wt% of 3YSZ nanoparticles (sample III), (e) KR7 with 0.5 wt% of 3YSZ nanoparticles (sample III), and (f) Mobil 1 with 0.5 wt% of 3YSZ nanoparticles (sample III).

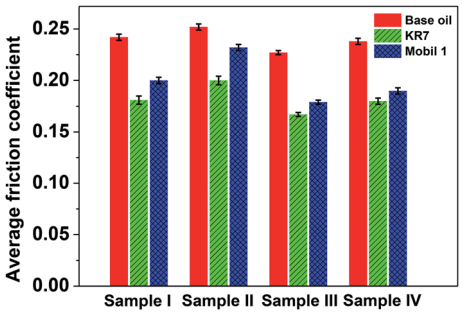

Fig. 10 Average friction coefficients of various 3YSZ nanoparticles in the base mineral oil, KR7, and Mobil 1 with a fixed concentration of 0.1 wt%. The tests were performed under a load of 80 N and a rotational speed of 400 rpm for 1 h.

coexisting tetragonal and monoclinic phases in this study are much harder and more stable than the non-stabilized ZrO_2 nanoparticles with only the monoclinic phase reported in the literature.[16] In this study, severe polishing occurred at the friction interfaces during the initial stages of four-ball testing as the nanoparticle clusters disaggregated, leading to a huge increase in WSD and a reduction in friction coefficient later on. As for the commercial formulated oils, the addition of 0.1 wt% of our 3YSZ nanoparticles helped reduce the wear for both KR7 and Mobil 1 by 15–20%. When the concentration of 3YSZ nanoparticles increased to 0.5 and 1.0 wt%, the KR7 oil retained a similar wear rate, while the WSD of the Mobil 1 oil increased by 20–25%. This result demonstrates that our 3YSZ nanoparticles are better at reducing wear in KR7 than in Mobil 1, and the formulation may be the key to the tribological performance of lubricating oils containing nanoparticles.

Finally, we dispersed all the prepared 3YSZ nanoparticles (samples I–IV) in base mineral oil, KR7, and Mobil 1 at a fixed concentration of 0.1 wt% and tested the tribological performances under a load of 80 N and a rotational speed of 400 rpm for 1 h. Fig. 10 compares the average friction coefficients of the above samples. All the oil media containing sample III exhibited lower friction coefficients than the corresponding oils with other 3YSZ nanoparticles. This suggests that the 3YSZ nanoparticles synthesized with the aid of polyether amine surfactant show better tribological properties in both base mineral oil and commercial formulated oils compared to the nanoparticles prepared with other surfactants or without surfactant. In addition, controlling the nanoparticle size and size distribution is the key to obtaining high-performance lubricating oils containing 3YSZ nanoparticles.

4. Conclusions

We have systematically investigated the syntheses of 3YSZ nanoparticles in a precipitation–calcination approach using various surfactants. The results of nanoparticle characterization show that the use of polyether amine as a surfactant during the synthesis favors the formation of stabilized zirconia nanocrystals with coexisting tetragonal and monoclinic phases compared to the syntheses without any surfactant and those using polyethylene glycol or polyvinyl pyrrolidone as surfactant. The 3YSZ nanoparticles prepared with the addition of polyether amine are also smaller in size and more uniform than those synthesized with other surfactants and without surfactant. The tribological four-ball measurements show that the 3YSZ nanoparticles are effective at reducing the friction coefficient of the base mineral oil, although they cause a significant increase in wear rate. The 3YSZ nanoparticles prepared in the current study have much better friction-reduction and anti-wear performance in commercial formulated lubricating oils, as compared to their performance in the base mineral oil, at the optimal nanoparticle concentration of ~0.1–0.5 wt%. The tribological comparisons between different oil media and different nanoparticles illustrate that the nanoparticle sizes and size distributions, their dispersions, and the oil formulations are all crucial in designing nanoparticle-bearing lubricating oils. The detailed relationship between the lubricating formulations and 3YSZ nanoparticles, as well as other lubricating nanomaterials, is under current investigation.

Author contributions

The experimental work was conducted by DL and YX. DS supervised the work. YS helped with the nanoparticle dispersion work and some of the tribological tests. The manuscript was written by DL and DS. All authors have given approval to the final version of the manuscript.

Conflict of interest

The authors declare no competing financial interest.

Acknowledgements

This work was supported by start-up funding from the Southern University of Science and Technology (SUSTech) and "The Recruitment Program of Global Youth Experts of China", the Foundation of Shenzhen Science and Technology Innovation Committee (Grant No. ZDSYS20140509142721431, JCYJ20120830154526538, JCYJ20160315164631204, and KQTD20140630110339343), and NSFC-21306077. YX acknowledges the provincial "Innovation and Entrepreneurship Training Funding for Undergraduates" from SUSTech. TEM was performed at the Life Science Research Facility of the Materials Characterization Center in SUSTech under the assistance of Ms Zan Li and Mr Dongsheng He.

References

1 B. Bhushan, J. N. Israelachvili and U. Landman, *Nature*, 1995, **374**, 607–616.
2 Q. J. Xue, W. M. Liu and Z. J. Zhang, *Wear*, 1997, **213**, 29–32.
3 Z. J. Zhang, Q. J. Xue and J. Zhang, *Wear*, 1997, **209**, 8–12.
4 J. X. Dong and Z. S. Hu, *Tribol. Int.*, 1998, **31**, 219–223.
5 Z. S. Hu, J. X. Dong and G. X. Chen, *Tribol. Int.*, 1998, **31**, 355–360.

6 A. H. Battez, J. E. F. Rico, A. N. Arias, J. L. V. Rodriguez, R. C. Rodriguez and J. M. D. Fernandez, *Wear*, 2006, **261**, 256–263.
7 L. Joly-Pottuz, N. Matsumoto, H. Kinoshita, B. Vacher, M. Belin, G. Montagnac, J. M. Martin and N. Ohmae, *Tribol. Int.*, 2008, **41**, 69–78.
8 D. Kim and L. A. Archer, *Langmuir*, 2011, **27**, 3083–3094.
9 T. W. Scharf and S. V. Prasad, *J. Mater. Sci.*, 2013, **48**, 511–531.
10 Z. Tang and S. Li, *Curr. Opin. Solid State Mater. Sci.*, 2014, **18**, 119–139.
11 Y. Y. Wu, W. C. Tsui and T. C. Liu, *Wear*, 2007, **262**, 819–825.
12 S. Ingole, A. Charanpahari, A. Kakade, S. S. Umare, D. V. Bhatt and J. Menghani, *Wear*, 2013, **301**, 776–785.
13 T. Luo, X. Wei, X. Huang, L. Huang and F. Yang, *Ceram. Int.*, 2014, **40**, 7143–7149.
14 T. Luo, X. Wei, H. Zhao, G. Cai and X. Zheng, *Ceram. Int.*, 2014, **40**, 10103–10109.
15 A. Hernández Battez, R. González, D. Felgueroso, J. E. Fernández, M. del Rocío Fernández, M. A. García and I. Peñuelas, *Wear*, 2007, **263**, 1568–1574.
16 A. Hernández Battez, R. González, J. L. Viesca, J. E. Fernández, J. M. Díaz Fernández, A. Machado, R. Chou and J. Riba, *Wear*, 2008, **265**, 422–428.
17 Q. Chen, K. C. Chan and L. Liu, *Philos. Mag.*, 2011, **91**, 3705–3715.
18 Y. S. Wang, C. He, B. J. Hockey, P. I. Lacey and S. M. Hsu, *Wear*, 1995, **181–183**, 156–164.
19 C. F. Gutiérrez-González and J. F. Bartolomé, *Wear*, 2013, **303**, 211–215.
20 T. Sato and M. Shimada, *J. Mater. Sci.*, 1985, **20**, 3988–3992.
21 S. W. Lee, S. M. Hsu and M. C. Shen, *J. Am. Ceram. Soc.*, 1993, **76**, 1937–1947.
22 P. D. L. Mercera, J. G. van Ommen, E. B. M. Doesburg, A. J. Burggraaf and J. R. H. Ross, *Appl. Catal.*, 1991, **71**, 363–391.
23 C.-W. Kuo, Y.-H. Shen, F.-L. Yen, H.-Z. Cheng, I. M. Hung, S.-B. Wen, M.-C. Wang and M. Stack, *Ceram. Int.*, 2014, **40**, 3243–3251.
24 G. Dell'Agli and G. Mascolo, *J. Eur. Ceram. Soc.*, 2000, **20**, 139–145.
25 R. R. Piticescu, C. Monty, D. Taloi, A. Motoc and S. Axinte, *J. Eur. Ceram. Soc.*, 2001, **21**, 2057–2060.
26 C. Viazzi, J.-P. Bonino, F. Ansart and A. Barnabé, *J. Alloys Compd.*, 2008, **452**, 377–383.
27 H. S. Liu, T. S. Chin, L. S. Lai, S. Y. Chiu, K. H. Chung, C. S. Chang and M. T. Lui, *Ceram. Int.*, 1997, **23**, 19–25.
28 C.-W. Kuo, Y.-H. Shen, I. M. Hung, S.-B. Wen, H.-E. Lee and M.-C. Wang, *J. Alloys Compd.*, 2009, **472**, 186–193.
29 M. R. Álvarez, A. R. Landa, L. C. Otero-Díaz and M. J. Torralvo, *J. Eur. Ceram. Soc.*, 1998, **18**, 1201–1210.
30 W. Dongfang, L. Jian and M. Zhiyuan, *Wear*, 1993, **165**, 159–167.